

Correlations with sun yaw angle in Aqua MODIS calibration coefficients (Incomplete Draft !)

January 6, 2005

Gerhard Meister, NASA Goddard Space Flight Center , Code 970.2
(meister@simbios.gsfc.nasa.gov, 301-286-0758)

Contents

1	Abstract	1
2	Introduction	2
3	Sun yaw angle correlations in the m1 coefficients	2
4	Creation of new LUT	13
5	Vignetting function	20
6	Appendix A: Detector m1 ratios	23
7	Appendix B: LUT comparison	32

1 Abstract

This report describes the correlations with sun yaw angle in Aqua MODIS calibration coefficients (m1), their removal and the creation of a L1B calibration LUT with the corrected m1.

2 Introduction

This report uses the m1 measurements provided by MCST on 12/07/04 and the LUT V5.0.1.0. The m1s were calculated by MCST with the following formula:

$$m_1 = \frac{BRF_{SD} \cdot \cos(\theta_{SD})}{dn_{SD} \cdot d_{Earth-Sun}^2} \cdot \Delta_{SD} \cdot \Gamma \quad (1)$$

where Γ is the vignetting function. The m1 are used to derive the earth scene reflectance factors with:

$$\rho_{EV} \cdot \cos(\theta_{EV}) = m1 \cdot dn_{EV} \cdot d_{Earth-Sun}^2 \quad (2)$$

see [1] for more explanations. In this report, the sun yaw angle will usually be referred to as beta (β) angle.

3 Sun yaw angle correlations in the m1 coefficients

3.1 Detector ratios

Fig. 1 shows the m1 for detectors 10 and 1 for bands 8, 16, and 18. It can be seen that the detector ratios for bands 8 and 16 have a strong correlation with the beta angle (ratio varies by about 0.5% with β angle), whereas band 18 does not have a similar correlation. As can be seen in appendix A, all the m1 detector ratios from bands that were measured with a screen (bands 8-16) have a similar correlation, but the bands that were measured without a screen do not have a similar correlation with β angle.

For those bands where the correlation is linear (especially bands 11 and 12), it can be seen that even the secondary maxima in the β angle around days 450 and 850 are present in the detector ratio, see Fig. 2. This shows that the detector ratio pattern is not seasonal, but directly related to the β angle. Furthermore, the occurrence of the pattern is not determined by wavelength (bands 1-4 do not have the pattern, and their wavelengths are bracketed by bands 8-16) or position on the focal plane (neither bands 1-4 in the center of the focal plane nor bands 17-19 on the edges of the focal plane have the pattern, bands 8-16 are located in between these bands, see Fig. 5). It is thus unlikely to be caused by earthshine.

The most likely candidate for producing the pattern is the solar diffuser screen, because this pattern exists only in the bands that were measured with the screen. Ideally, the vignetting function should remove this pattern. Unfortunately, the detector averaged vignetting function used in LUT V5.0.1.0 does not do this. In section 5.3 below, it will be shown that a detector dependent vignetting function derived from either the yaw maneuver (by MCST) or from on-orbit calibration events (derivation presented in section 5) reduces the ratio pattern.

The bands that were measured with the screen are also the most sensitive bands, thus it could be argued that not the screen, but the sensitivity of the band is the reason for the occurrence of this

pattern. The β angle is correlated with the solar zenith angle on the solar diffuser, see Fig. 3. The irradiance on the solar diffuser is proportional to the cosine of the solar zenith angle on the solar diffuser. Therefore, the larger the β angle, the lower the radiance reflected from the solar diffuser. However, there is no reason why detector 10 should be affected differently than detector 1, thus the vignetting function remains the most likely source for the detector 10/1 pattern.

The ratio is plotted versus β angles for all ocean bands in Fig. 4. It can be seen that the ratio is quite linear for bands 11 and 12 (and 13 to some extent), but has a clear minimum around $\beta = 20^\circ$ for the other bands. Bands 11-13 are on one side of the focal plane, bands 8-10 and 14-16 are on the other side of the focal plane, see Fig. 5. This shows that the exact β dependence of the detector ratio depends on the position on the focal plane of the respective bands. The minimum at $\beta = 20^\circ$ is most pronounced for band 16, the band furthest away from bands 11 and 12.

So far in this report, only the detector ratios of ocean bands have been shown to have a β angle dependence. There is no dispute about these results, only simple ratioing was used to derive them. The author's conclusion that the screen (vignetting function) is the cause for this dependence has not been proven, but it is by far the most likely explanation.

In the following section, a more sophisticated approach will be used to show that not only the detector ratios, but also the ocean bands themselves have a β angle dependence.

3.2 Band dependence

In order to derive the β angle dependence of the m1 for a specific band, an estimate of the true m1 is needed. The ratios of the m1 and this first estimate will be used to investigate the β angle dependence. The derived β angle dependence will then be used to correct the m1. The resulting m1 will obviously be very similar to the original estimate. This is a weakness of the method presented here. However, it will be shown that the derived β angle dependence has some common features with the undisputable results of section 3.1, which is an indication that the approach indeed characterizes the true β angle dependence.

The underlying cause for the band dependence on the β angle is not clear. For the case of the detector ratios, it was shown that the pattern in the detector ratio does not occur in those bands measured without the screen, thus it could be concluded that the vignetting function is the cause. For the band dependence, it has not yet been investigated whether there are correlations with β angle, and whether they are similar to those in the ocean bands. However, the similarities between the conclusions regarding the detector ratio and the band dependence indicate that the underlying cause might be identical.

Another potential cause is that an inaccurate characterization of the BRDF of the solar diffuser introduces the band dependence on β angle. This is unlikely to be the only reason for the band dependence, because the band dependence can be characterized better as a function of the position of the band on the focal plane than as a function of wavelength, see below. Still, it might be a significant contribution.

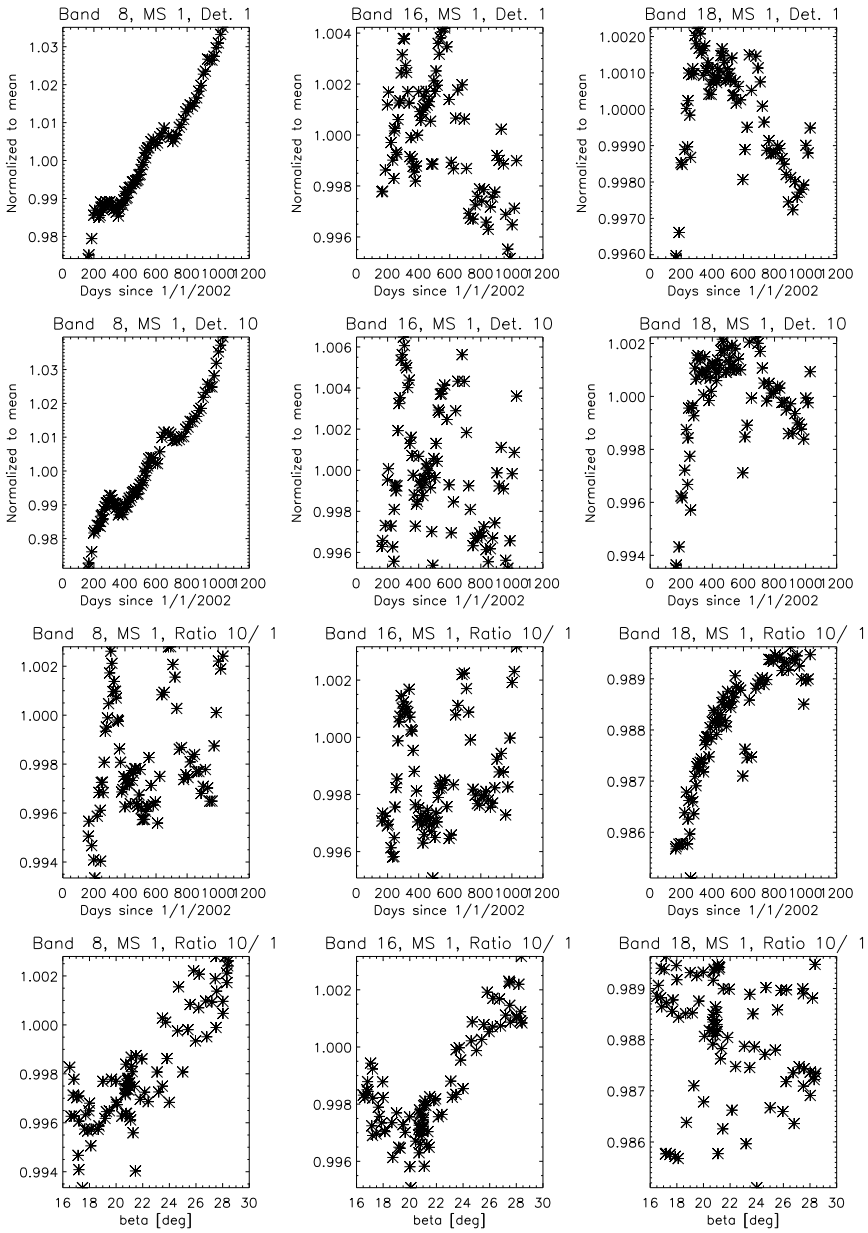


Figure 1: MODIS Aqua m1 for band 8 (left column), band 16 (middle column) and band 18 (right column). Top row: m1 for detector 1. Second row: m1 for detector 10. Third row: m1 of detector 10 divided by m1 of detector 1. Forth row: same as third row, but plotted versus β angle.

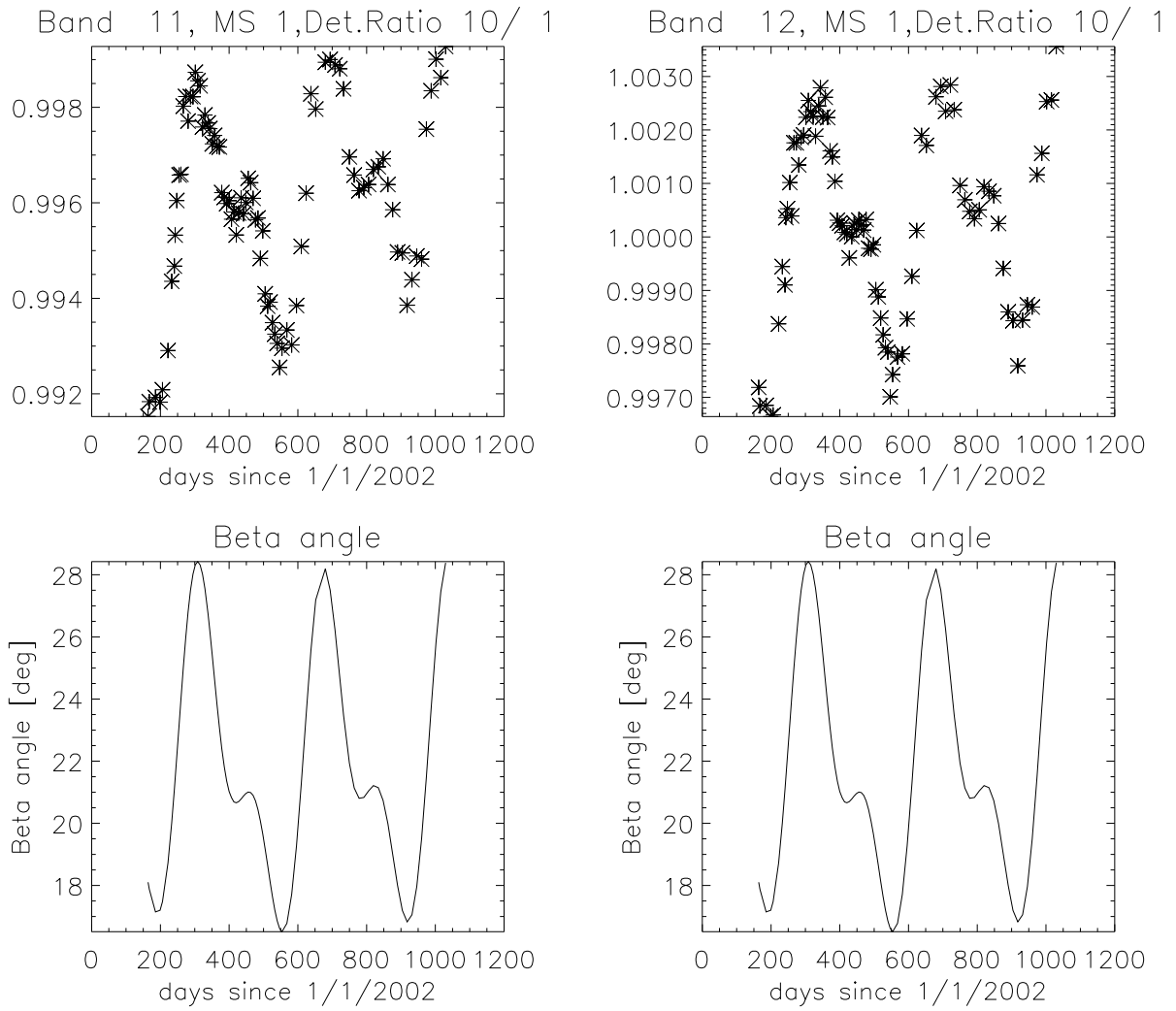


Figure 2: Top row: MODIS Aqua m1 detector 10/1 ratio for band 11 (left) and band 12 (right). Bottom row: β angle versus time.

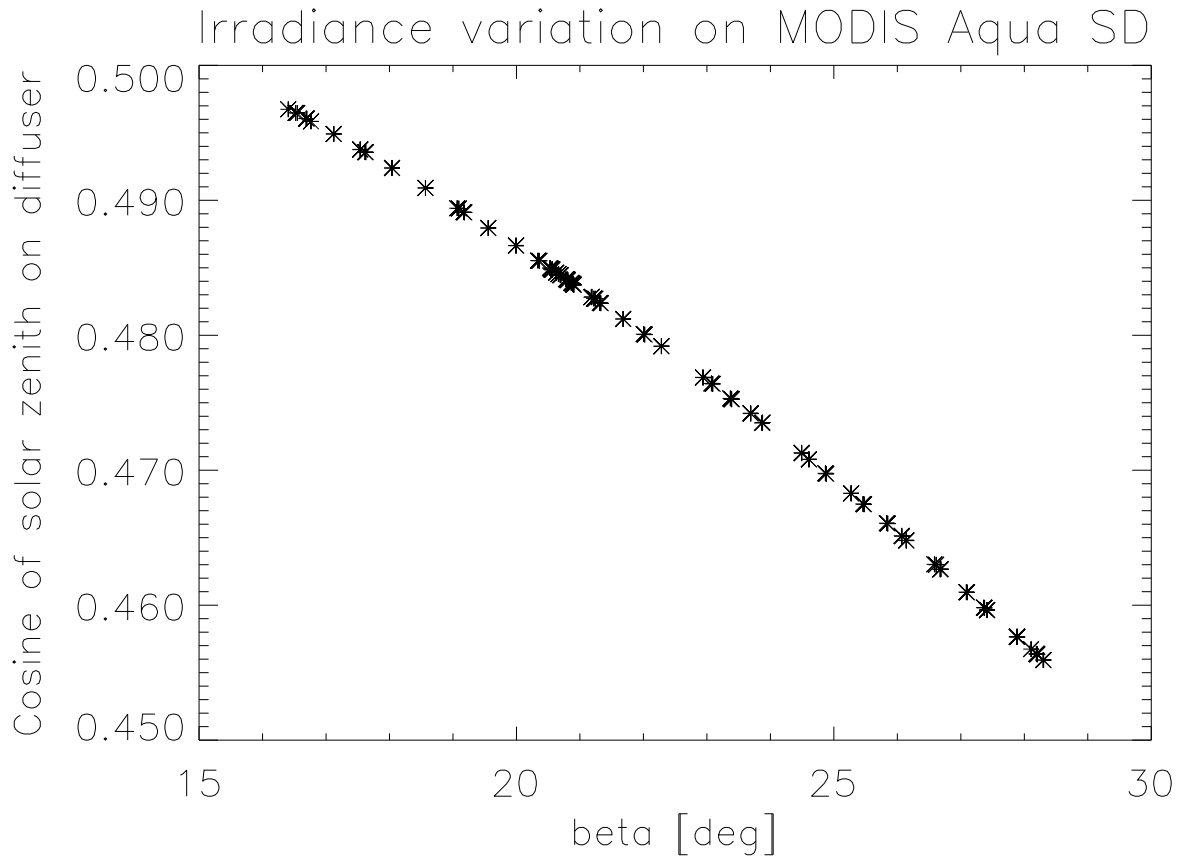


Figure 3: The cosine of the solar zenith angle on the solar diffuser versus β angle varies by about 10% for the on-orbit calibration events of MODIS Aqua.

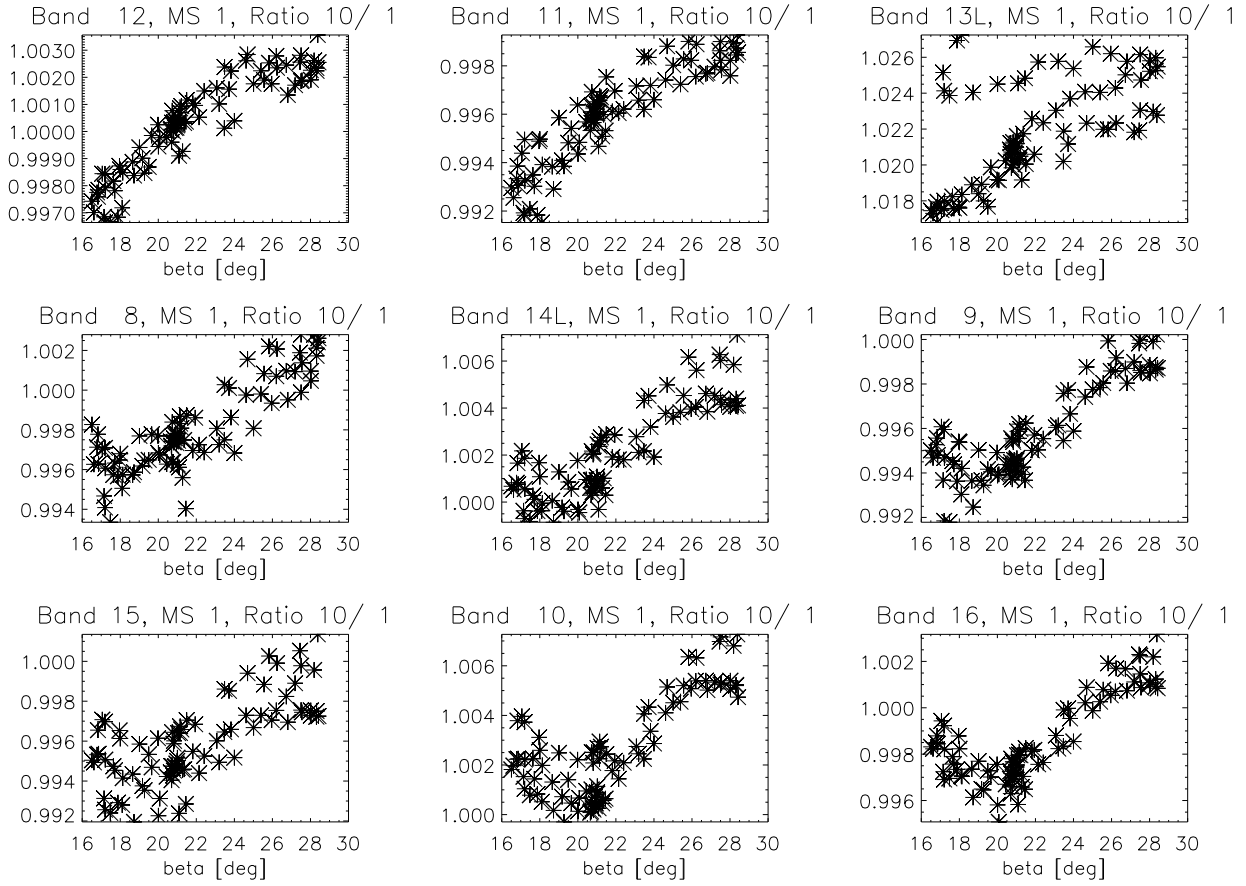


Figure 4: Detector 10/1 ratio for ocean bands versus β angle. The bands are plotted in the order of their position on the focal plane, see Fig. 5.

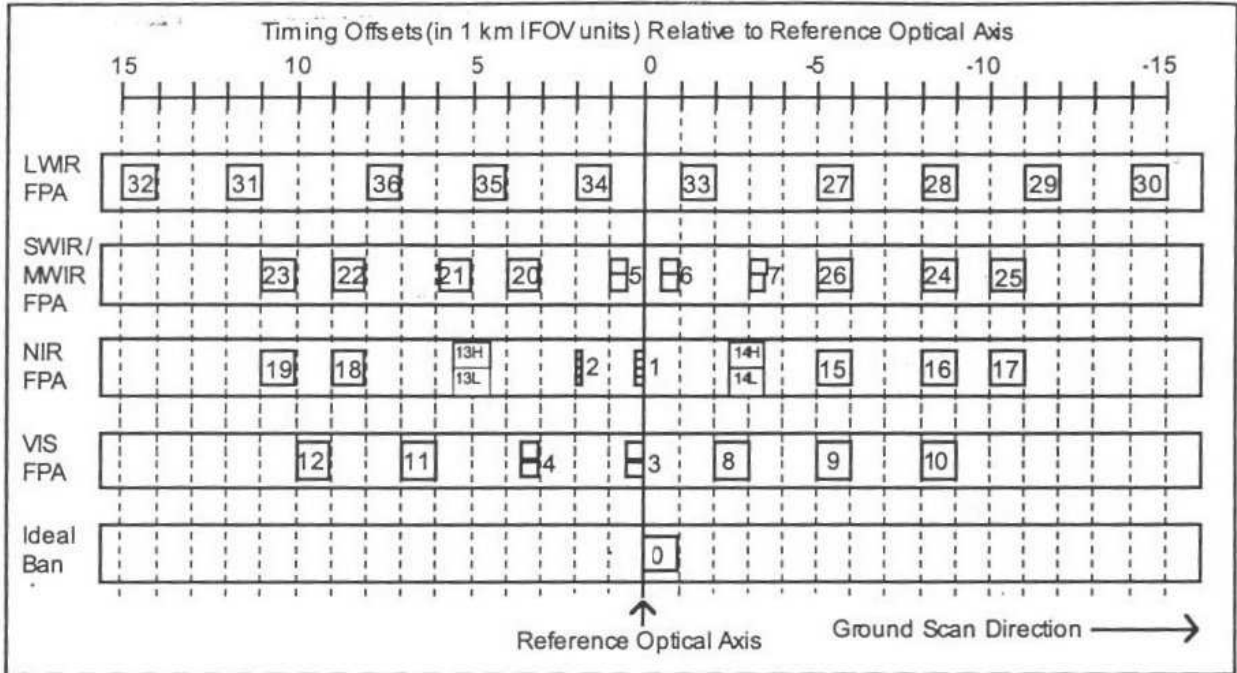


Figure 3-11. Offset of Each Band Relative to the Reference Optical Axis

Figure 5: Layout of the MODIS focal planes[2].

3.2.1 Analytical functions for detector degradation

There are several options to arrive at a first estimate of the m1. Almost all involve the choice of an analytical function (or a combination of analytical functions), like exponentials, logarithms, polynomials, trigonometric functions, etc. The degradation of the SeaWiFS sensor is well understood[3], it roughly follows an exponential degradation. (In effect, the SeaWiFS time series is so long (more than 6 years) that the assumption of two simultaneous exponentials produces a slightly better agreement with the measured data for some bands.) Johnston ([4]) presents results from a laboratory study on the degradation of silicon detectors under proton irradiation, which is the dominant source of ionizing radiation assuming adequate shielding of the electronics within the spacecraft. The plots in [4] suggest that an exponential degradation is indeed a good approximation. The exponential function in the form used for SeaWiFS:

$$f(t) = a_0 - a_1 \cdot (1 - \exp -a_2 \cdot t), \quad t = \text{time} \quad (3)$$

has the advantage of having only 3 free parameters (a_0, a_1, a_2). In this report, an exponential function as in eq. 3 will be used to derive the first estimate for the m1. A set of a_i will be fitted for each band, detector, and mirror side.

In effect, an increasing m1 signifies a degrading sensor, see eq. 2. The exponential in eq. 3 decreases with time for positive a_2 . Thus f will be fitted to g , the reciprocal of the m1:

$$g(t) = \frac{1}{m_1(t)} \quad (4)$$

It is understood that the assumption of an exponential degradation may not work. In particular, MODIS Terra has shown significant deviations from an exponential degradation. In effect, even on MODIS Aqua, band 13 is becoming more sensitive with time, which defies the concept of degradation. No completely satisfying explanation has been found for the odd behaviour of band 13, but it is possible that a trend in the electronics, the filter transmittance or some other unknown effect is causing this behaviour. Fortunately, so far the m1 trends in the remaining MODIS Aqua bands can be relatively well described by a decaying exponential, as can be seen in Fig. 6.

3.2.2 Ratios to exponential function

The ratios r of the measured m1 and the exponential function are defined here as

$$r = \frac{1/f}{m_1} \quad (5)$$

with f from eq. 3, and are shown in Fig. 7, plotted versus the β angle. It can be seen that except for band 8, there is an obvious, band specific pattern. A polynomial $p(\beta)$ of third order,

$$p(\beta) = \sum_{i=0}^{i=3} p_0 \cdot \beta^i \quad (6)$$

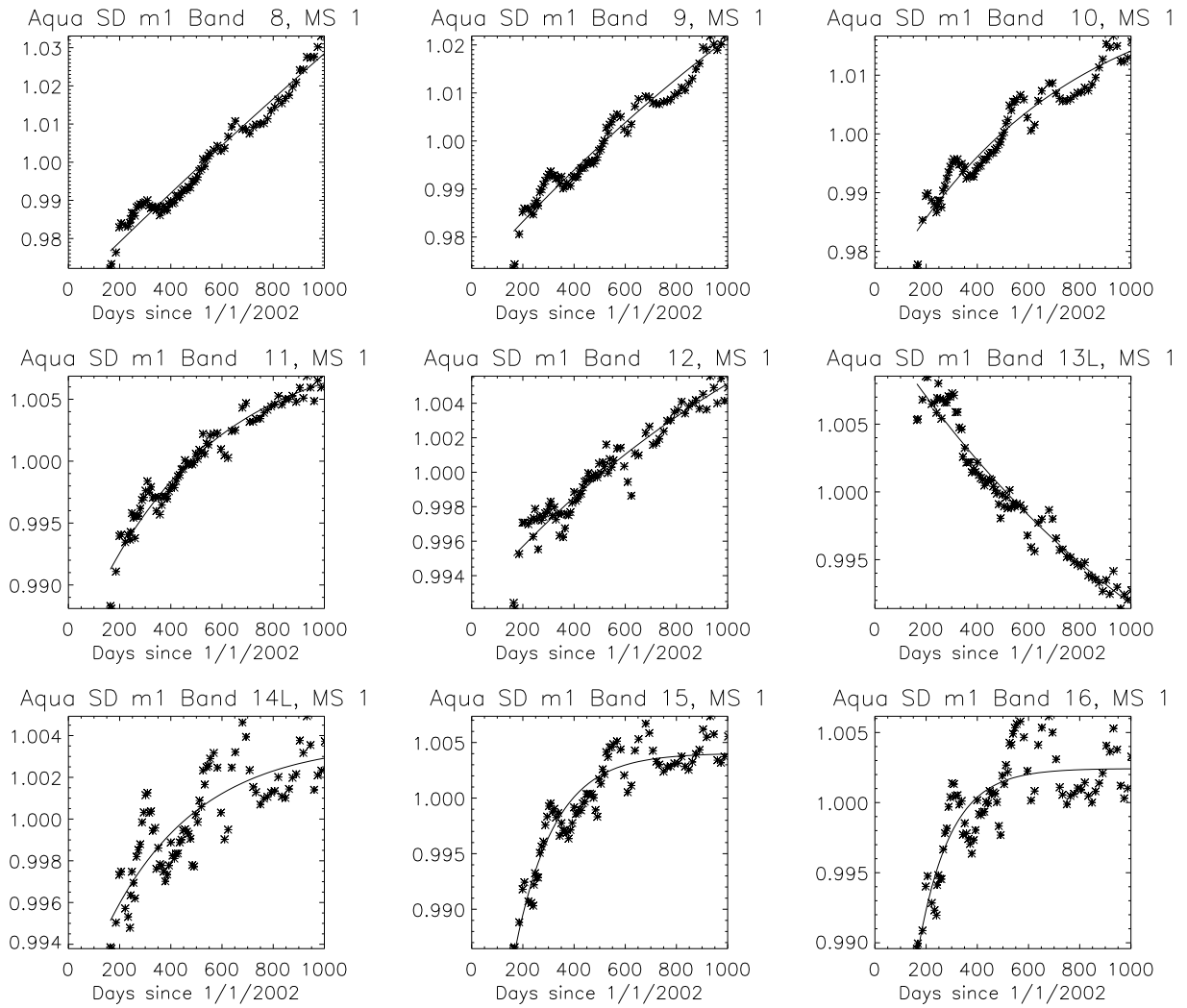


Figure 6: The stars show the m1 measurements for detector 5 for the ocean color bands as a function of time. The solid line shows a fit of equation 3 to the data (after inversion, see eq. 4).

was fitted to the ratios r and is shown as the solid line in Fig. 7. It can be seen that bands 11 and 12 have a similar pattern (constant for β angles less than about 25° , then decreasing), but their pattern is opposite to the pattern of the bands for the other side of the focal plane, (8-10, 14-16), which have a clear maximum around $\beta \approx 22^\circ$. Thus we see again that the β angle dependence differs for the different sides of the focal plane, the same result we arrived at when investigating the detector ratios (section 3.1).

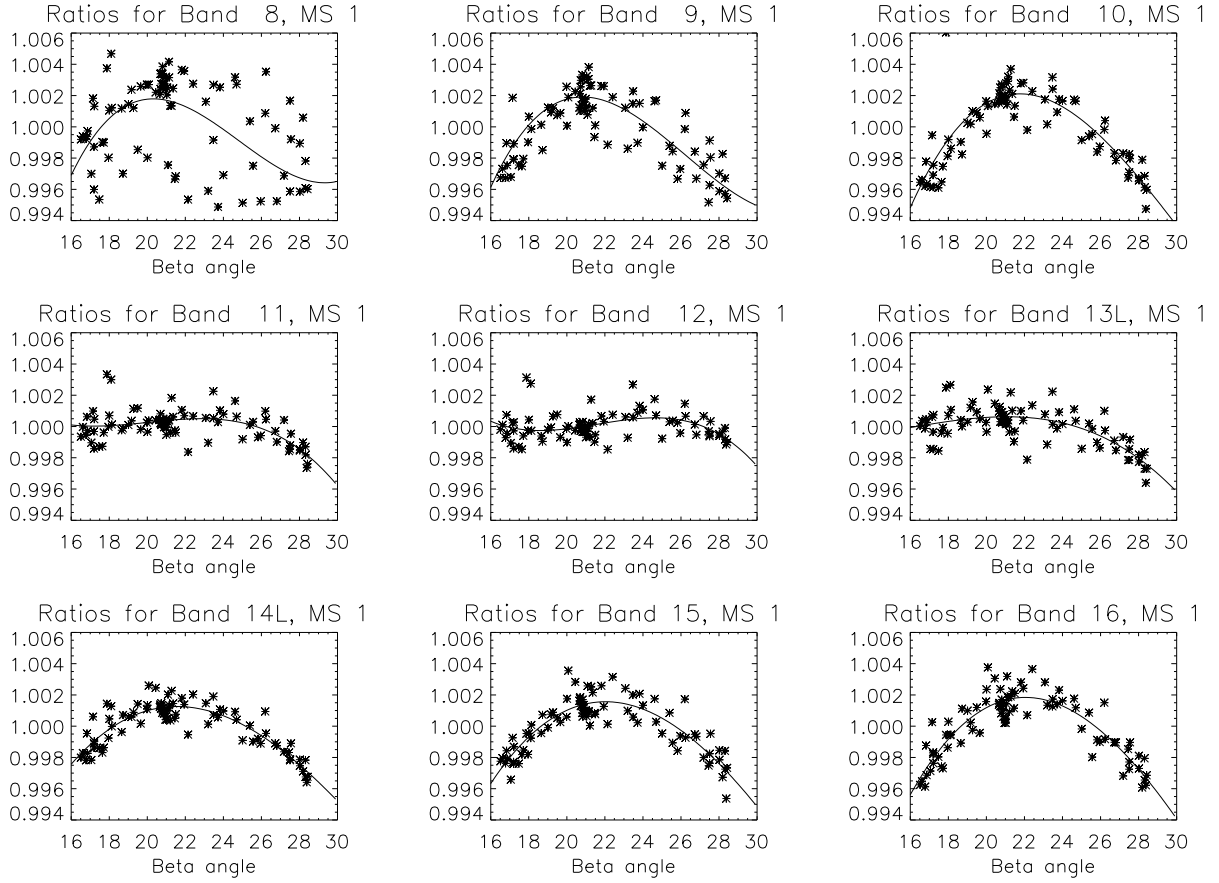


Figure 7: The stars show the ratios r (eq. 5) of the m1 measurements to the exponential fit for the ocean bands, detector 5, plotted versus the β angle. The solid line shows a third order polynomial of the β angle fitted to the ratios.

4 Creation of new LUT

We do not believe that the β angle dependence in the m1 measurements is a sign of a detector sensitivity that is proportional to the β angle. We believe that the β angle dependence is a calibration artifact, thus it needs to be removed from the m1 calibration coefficients. It could be argued that the MCST approach of fitting an analytical function to the m1 that depends only on time and not on the β angle effectively removes the β angle correlation. By comparing the predictions of a LUT derived by MCST and a LUT derived with the method described below, it can be seen that in some cases it is advantageous to remove the β angle dependence before fitting an analytical function.

This is demonstrated in Figs. 8 and 9. The red lines in these two figures show the m1 from the LUTs, the stars show the m1 measurements. For both LUTs, the last 3 measurements were not available at the time of the creation of the LUT (m1 measurements are usually scheduled every two weeks for MODIS Aqua). It can be seen that the red line in Fig. 9 agrees better with the last 3 measurements than the red line in Fig. 8, especially for bands 8 and 11. The plots were created in the middle of 2004 with the then current LUTs, the blue line is from a previous LUT that is not necessary for the argument made here. This is the only time this has been investigated, for other cases the conclusion may be opposite.

4.1 β angle dependence removal

The β angle dependence can be removed from the measured m1, $m_1^{\text{meas.}}$, by defining modified m1, $m_1^{\text{mod.}}$, as

$$m_1^{\text{mod.}} = m_1^{\text{meas.}} \cdot p(\beta) \quad (7)$$

where $p(\beta)$ is taken from eq. 6. The β angles for the m1 measurements were interpolated from a dataset provided by Fred Patt. Then, the $m_1^{\text{mod.}}$ are used as in eq. 4 to calculate

$$g^{\text{mod.}}(t) = \frac{1}{m_1(t)^{\text{mod.}}} \quad (8)$$

The values $g^{\text{mod.}}(t)$ are used to calculate new coefficients a_i for an exponential function $f^{\text{new}}(t)$ as in eq. 3. New m1, $m_1^{\text{new}}(t)$, are calculated with

$$m_1^{\text{new}}(t) = \frac{1}{f^{\text{new}}(t)} \quad (9)$$

and written into the reflective L1b LUT. A comparison of the modified measurements $m_1^{\text{mod.}}$ and the fitted m_1^{new} is shown in Fig. 10. It is remarkable how smooth the $m_1^{\text{mod.}}$ are. The ratios of the $m_1^{\text{mod.}}$ from the m_1^{new} are shown in Fig. 11. The overall agreement is excellent, the scatter is only about 0.1%. In band 8, there is a 1% variation at the beginning of the mission, the amplitude of this variation decreases with wavelength. Band 8 also has an increase of about 0.5% towards the end of the mission.

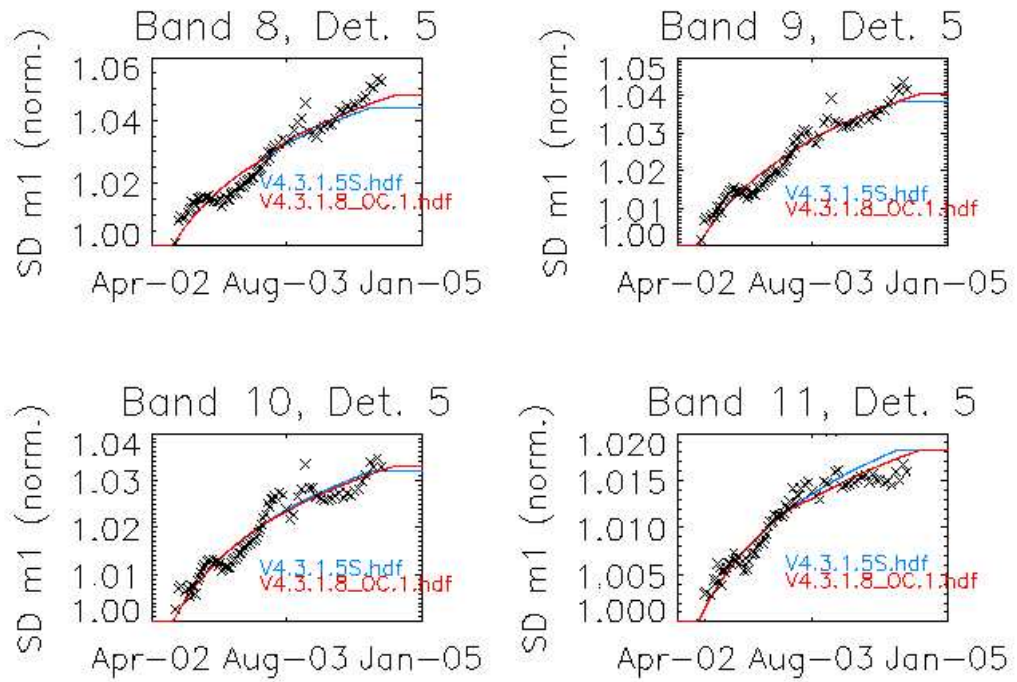


Figure 8: m1 measurements (stars) and m1 from LUT V4.3.1.8_OC.1 (red line), a LUT created by MCST with a logarithmic and polynomial fit for MODIS Aqua bands 8-11, detector 5, mirror side 1.

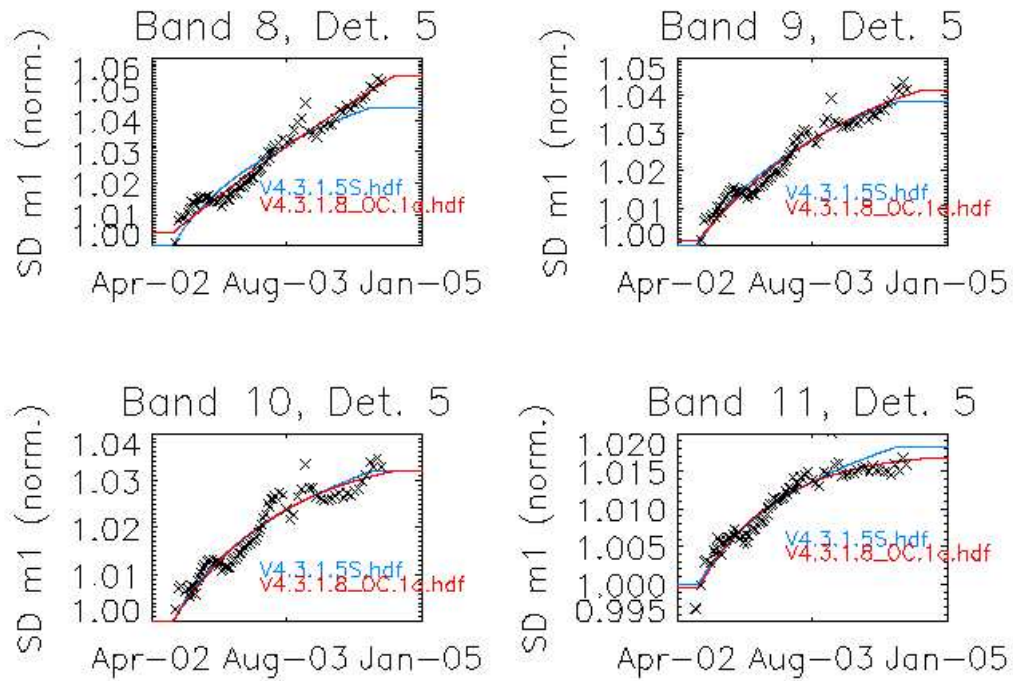


Figure 9: m1 measurements (stars) and m1 from LUT V4.3.1.8_OC.1a (red line), a LUT created with the approach described in this report for MODIS Aqua bands 8-11, detector 5, mirror side 1.

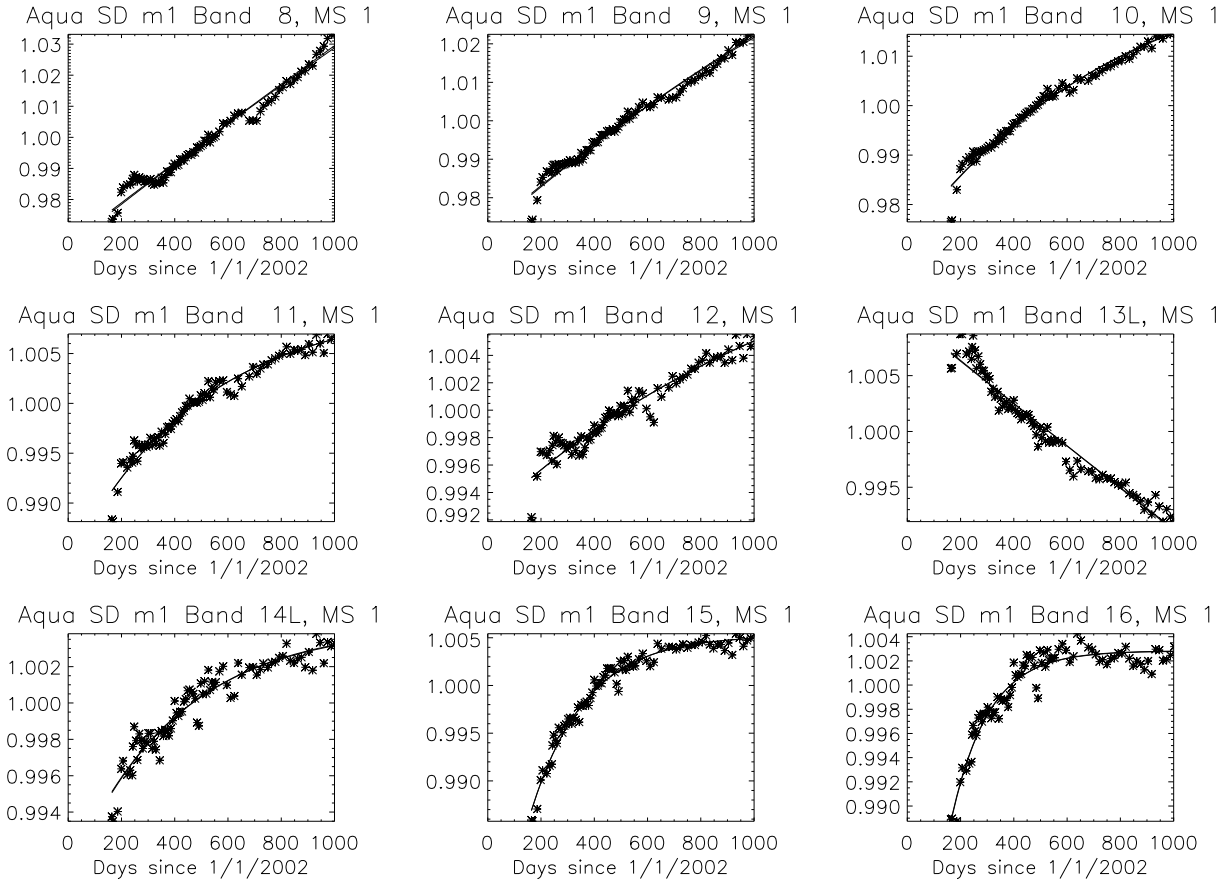


Figure 10: The stars show the m_1^{mod} . (see eq. 7) for detector 5 for the ocean color bands as a function of time. The solid line connects the fitted $m_1^{\text{new}}(t)$ (see eq. 9).

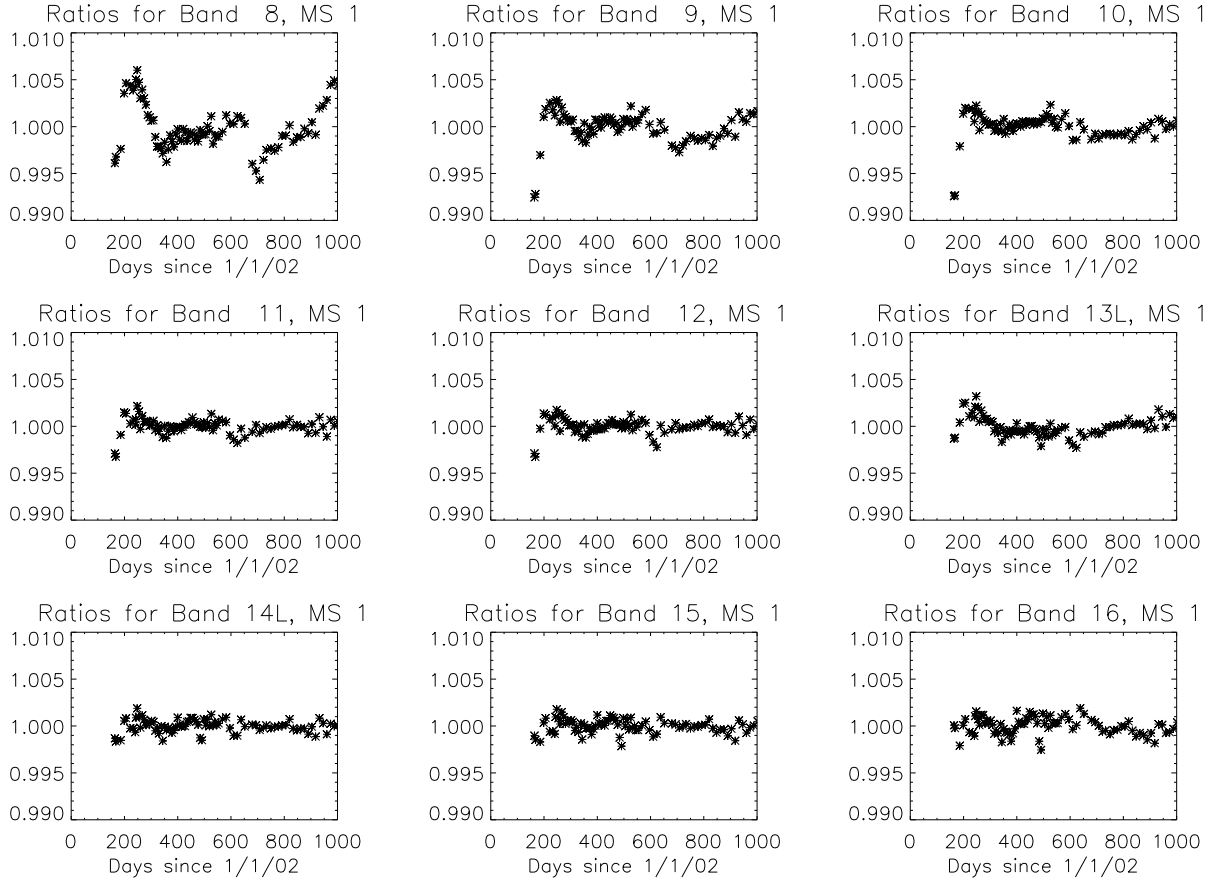


Figure 11: The stars show $m_1^{\text{mod.}}(t)$ divided by $m_1^{\text{new}}(t)$ for detector 5 for the ocean color bands as a function of time.

4.2 RVS adjustment

MCST derived the Aqua response versus scan (RVS) correction with lunar data, based on their m1 LUT. The RVS correction is applied relative to the m1,

$$m1(pixel, t) = \frac{m1^{LUT}(t)}{RVS(pixel, t)} \quad (10)$$

Assuming that the lunar trending by MCST is correct, the modifications to the m1 in section 4.1 will replace the $m1^{LUT}(t)$ with $m1^{new}(t)$, and produce incorrect m1 at the lunar viewing angle, see eq. 10. Thus the original $RVS(pixel, t)$ in the LUT must be replaced by

$$RVS^{new}(pixel, t) = RVS(pixel, t) \cdot \frac{m1^{new}(t)}{m1^{LUT}(t)} \quad (11)$$

The result for band 8 can be seen in Fig. 12: the modifications to the m1 at the SD viewing angle (top row) do not affect the m1 at the lunar viewing angle (bottom row). The other ocean color bands are shown in appendix B.

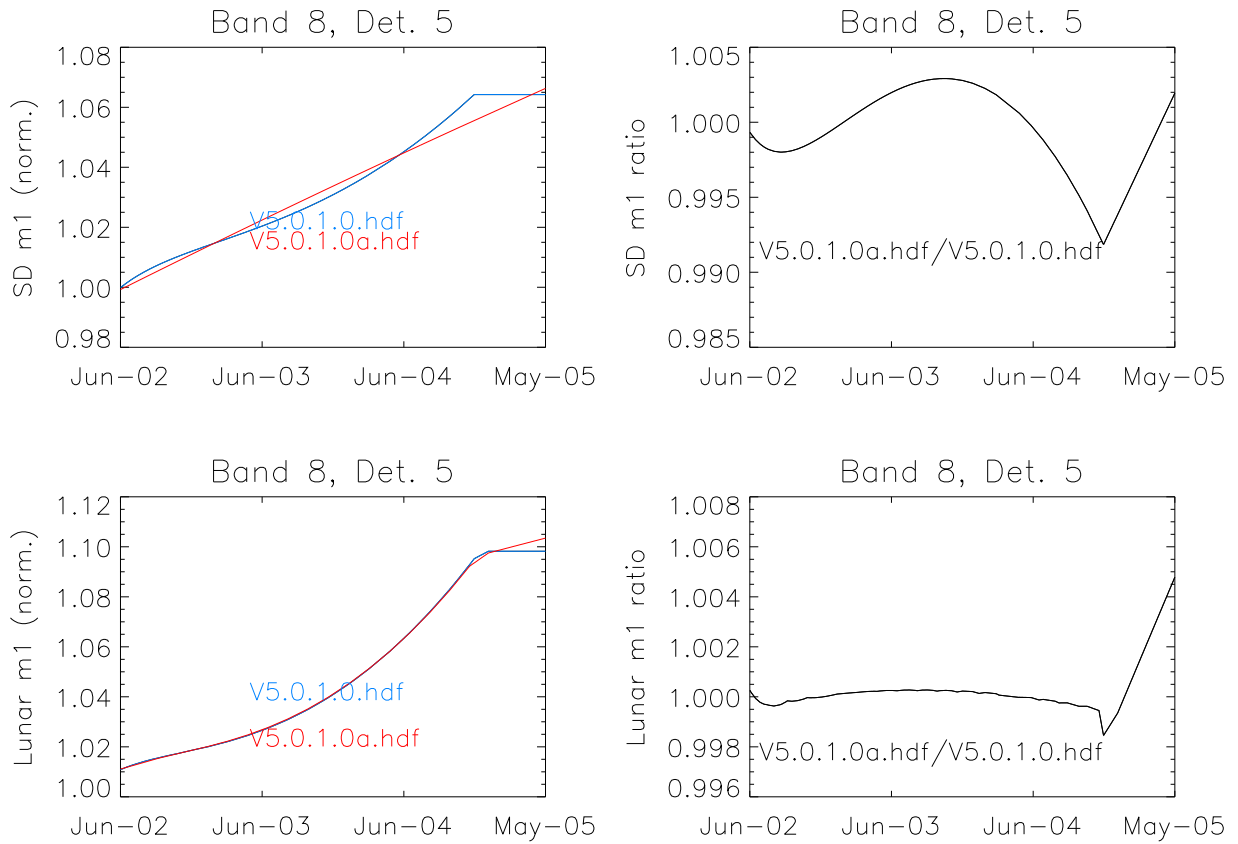


Figure 12: m_1 from original MCST LUT V5.0.1.0 (blue line) and modified LUT V5.0.1.0a (red line), for MODIS Aqua band 8, detector 5, mirror side 1. The plots on the left show the absolute values normalized to 1, the right side shows the ratio. The top plots show the m_1 at the solar diffuser viewing angle (these are the values stored in the LUT), the bottom plots show the m_1 at the lunar viewing angle (calculated with eq. 10). The m_1 in the original MCST LUT were not extrapolated beyond the last m_1 measurement, the plotting routine used in this figure assumed a constant m_1 for the extrapolation, which results in the horizontal blue line in the plots on the left, and produces the steep increase for the extrapolated values in the right plots.

5 Vignetting function

The work on sections 5.1 and 5.2 is still in progress, please proceed reading in section 5.3.

5.1 Calculation of the VF from SD calibration measurements

The biweekly SD calibration measurements were used to derive a VF. The no-screen measurements for non-saturating bands were divided by the screen measurements. These measurements are at least one orbit apart, but the change in β angle between the measurements is very small.

For bands with more than 10 detectors, the appropriate detectors were combined to simulate 10 detectors.

5.2 Comparison of results to yaw maneuver results

5.3 Detector ratio of m1 for detector dependent VF

MCST derived a detector dependent vignetting function from yaw maneuver data, averaging over bands 3, 4, 18, and 19. The m1 produced with this VF were provided in the LUT V4.3.1.11_OC. The detector 10/1 ratio for the ocean bands is shown in Fig. 13. It shows that the detector ratio pattern for bands 11 and 12 has been significantly reduced, compared to the m1 derived with a detector averaged VF. The original dependence of the bands 11 and 12 detector ratio on the β angle was an increase of about 0.6%, see Fig. 1. The variation in Fig. 13 is about 0.3% for bands 11 and 12, with no apparent trend. The reduction is less significant for the remaining bands. Note that bands 11 and 12 are from the same side of the focal plane as the bands used to derive the detector dependent VF (3,4, 18, 19), see Fig. 5. This indicates that

- It is indeed the VF that causes the detector ratio pattern, the true VF is detector dependent.
- The true detector ratio of the VF is band dependent.

Unfortunately, only one band is available from the other side of the focal plane to derive a VF, band 17. According to MCST, the measurements of this band are corrupted by pre-saturation problems.

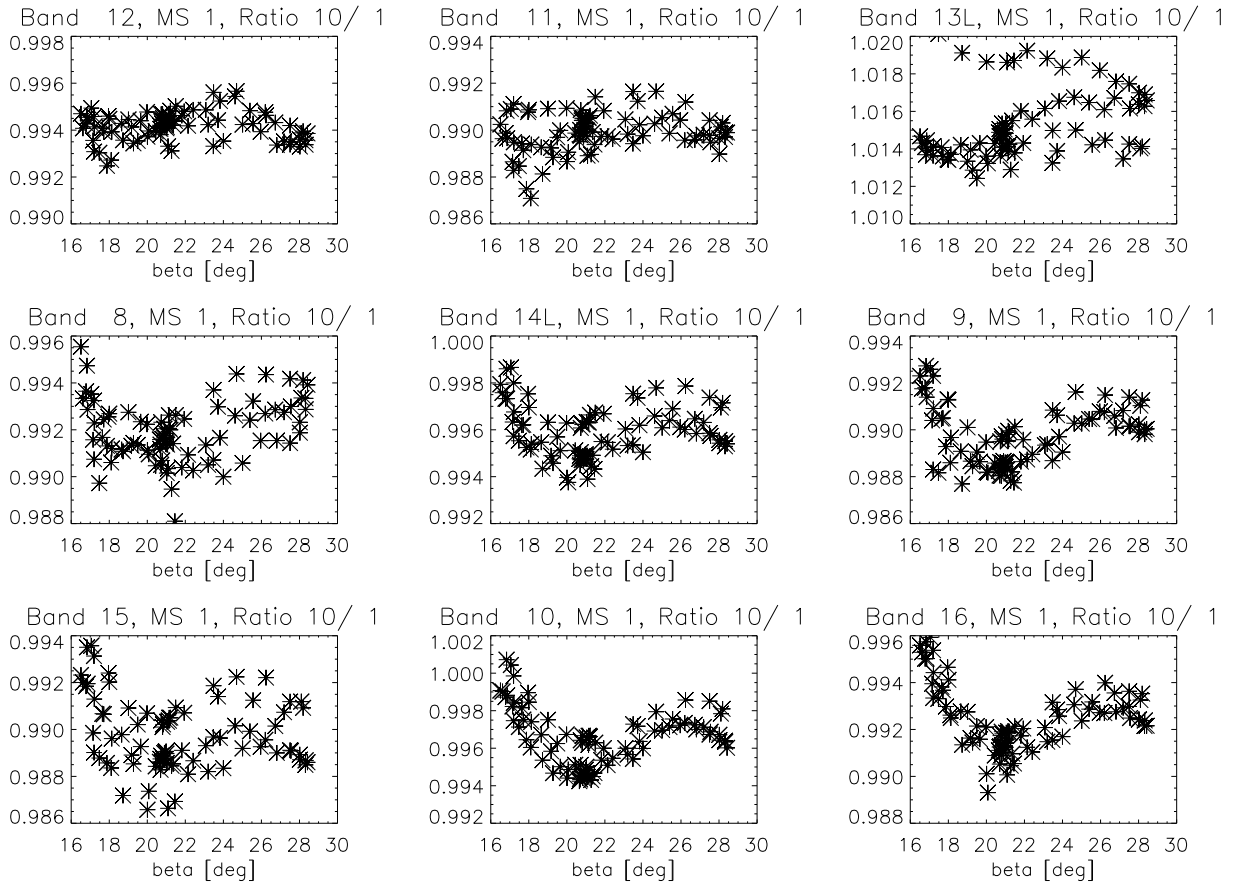


Figure 13: Detector 10/1 ratio for ocean bands versus β angle for the m1 calculated with the MCST detector dependent vignetting function (LUT V4.3.1.11_OC).

Acknowledgments

I want to thank my colleagues from MCST and OBPG for their support.

References

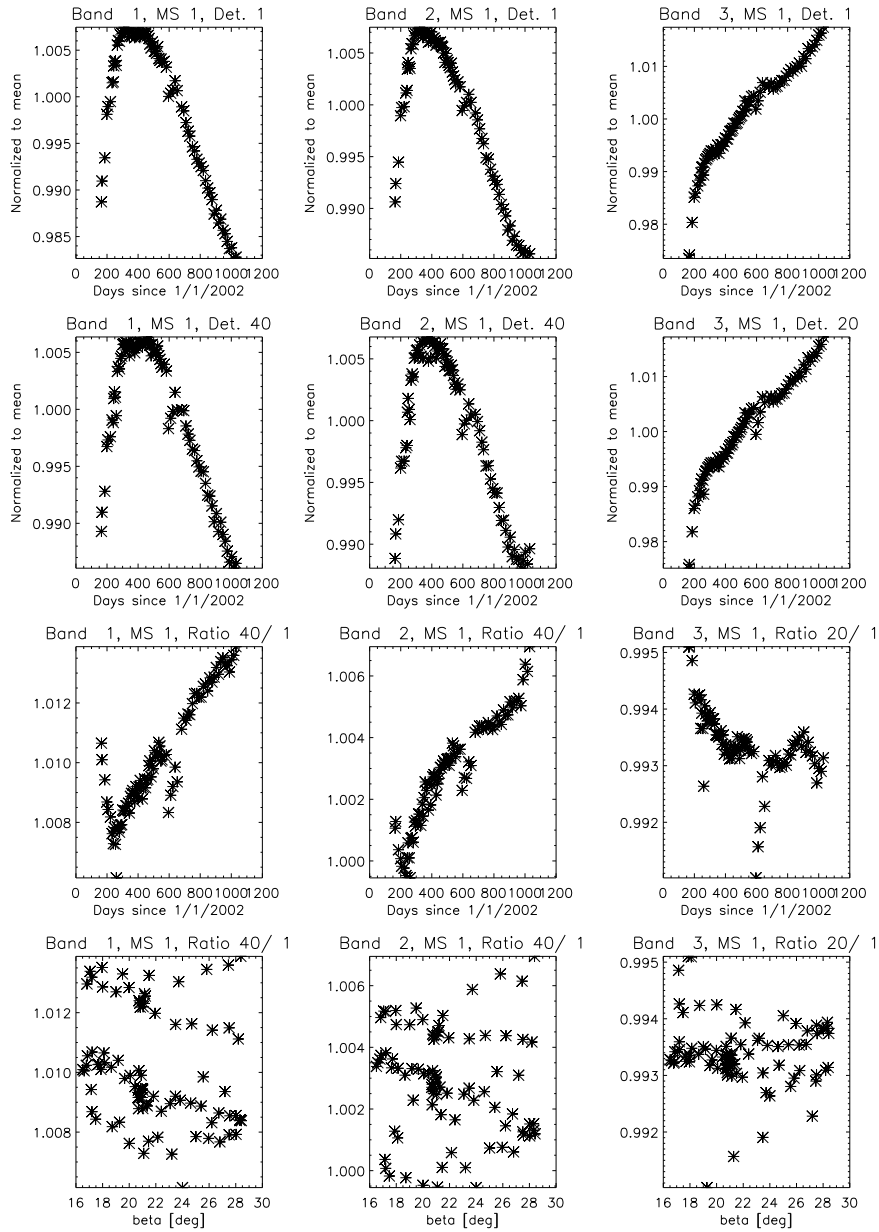
- [1] Xiong, X., Wu, A., Esposito, J.A., Sun, J., Che, N., Guenther, B., Barnes, W., Trending Results of MODIS Optics On-orbit Degradation, SPIE Vol. 4814, 337-346 (2002).
- [2] MODIS Level 1a Earth Location: ATBD, version 3.0, August 1997
- [3] Eplee, R.E., Barnes, R.A., Patt, F.S., Meister, G., McClain, C.R., SeaWiFS lunar calibration methodology after six years on orbit, SPIE Vol. 5542, 1-13 (2004)
- [4] A.H. Johnston, Radiation damage of Electronic and Optoelectronic Devices in Space, 4th International Workshop on Radiation Effects on Semiconductor Devices for Space Application, Tsukuba, Japan, October 2000

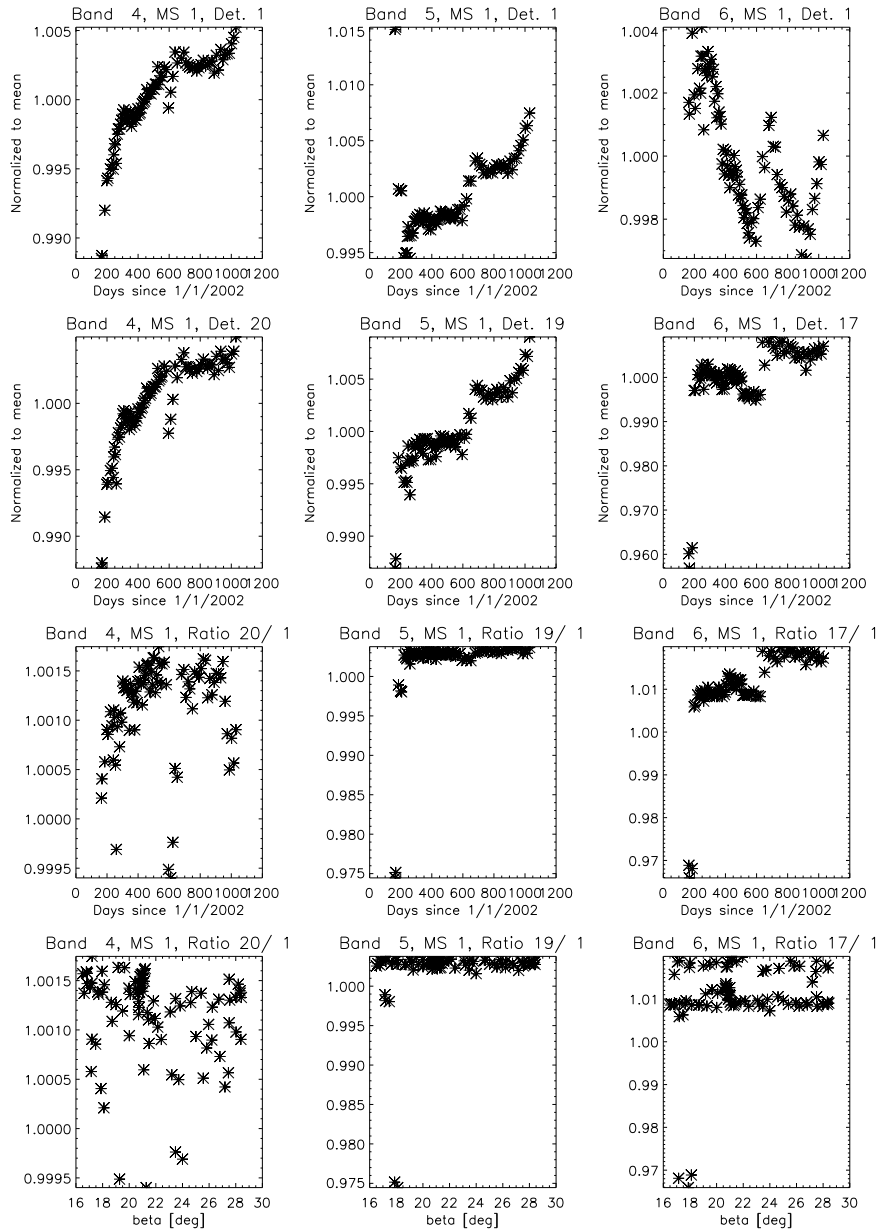
6 Appendix A: Detector m1 ratios

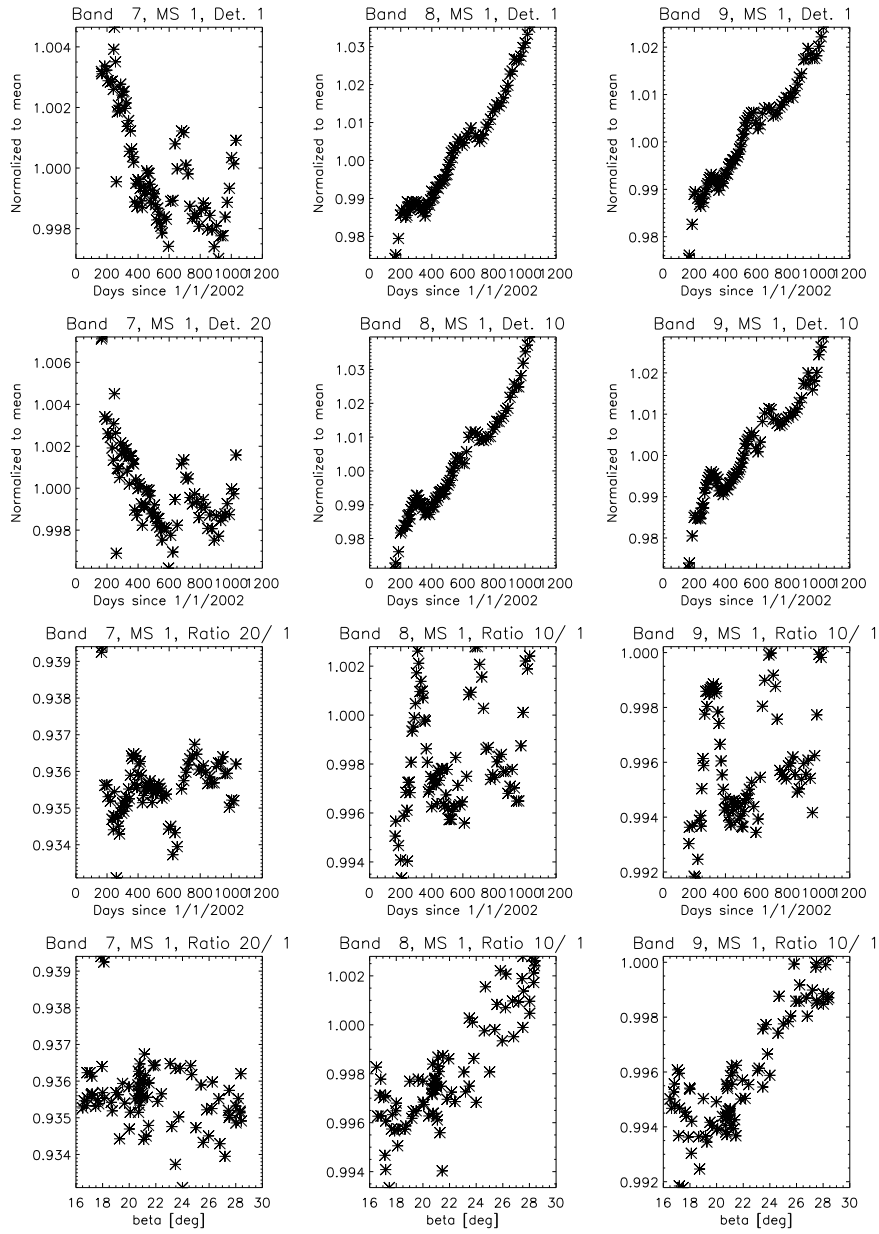
This appendix shows the measured m1 for the first and last detector (1 and 20 or 40 for bands 1-8, or neighboring detectors if these detectors are unusable, 1 and 10 for bands 8-19), the ratio versus time and the ratio versus β angle. The center wavelengths of the bands are given in table 1. The ocean bands have the detector ratio pattern with an order of magnitude of 0.5%. Only band 7 seems to have a similar pattern, but with a much smaller magnitude (0.03%), see plot versus time. However, when plotted against the β angle, the apparent correlation disappears.

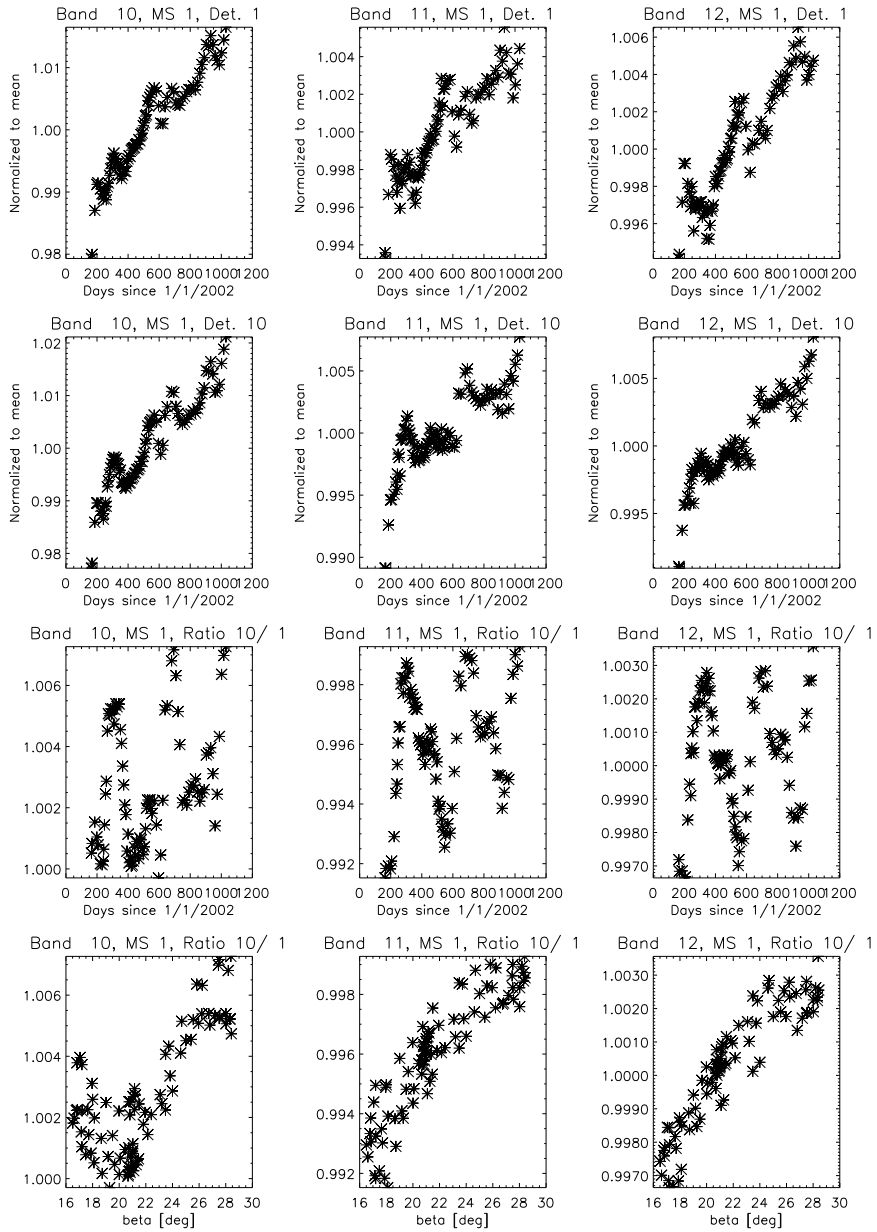
Table 1: Center wavelengths and bandwidths for the MODIS bands 1-19.

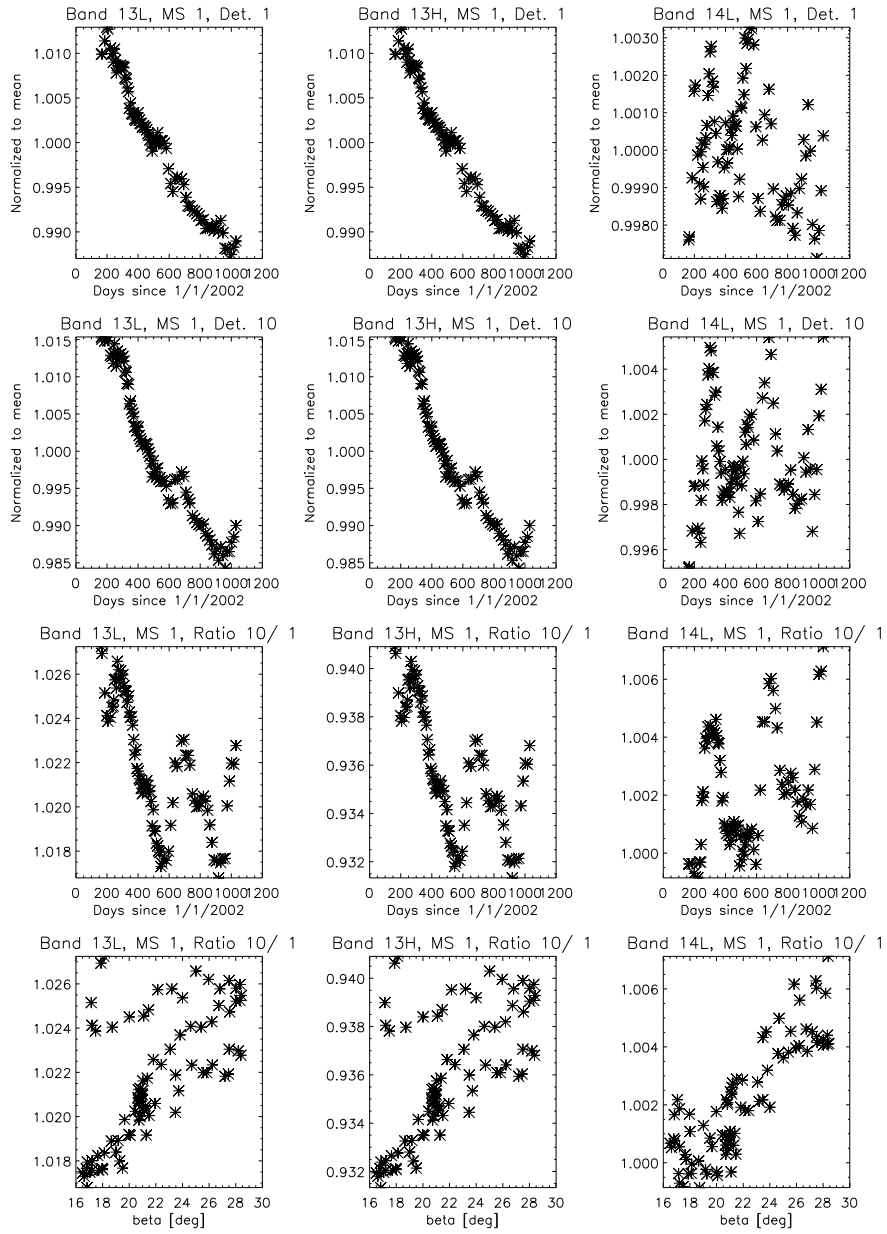
MODIS band number	MODIS center wavelength [nm]	MODIS bandwidth [nm]	Number of detectors
1	645	50	40
2	859	35	40
3	469	20	20
4	555	20	20
5	1240	20	20
6	1640	24	20
7	2130	50	20
8	413	15	10
9	443	10	10
10	488	10	10
11	531	10	10
12	551	10	10
13L/13H	667	10	10
14L/14H	678	10	10
15	748	10	10
16	870	15	10
17	905	30	10
18	936	10	10
19	940	50	10

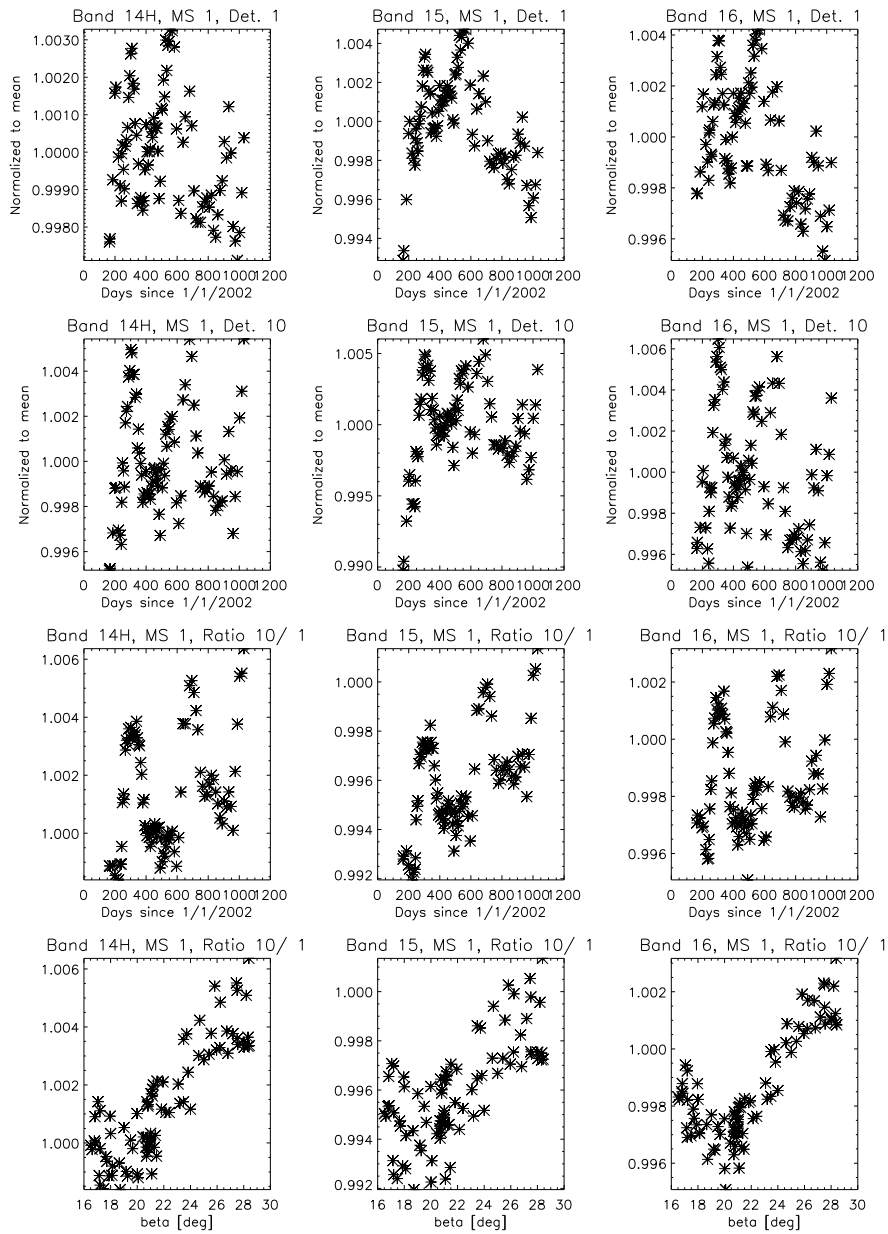


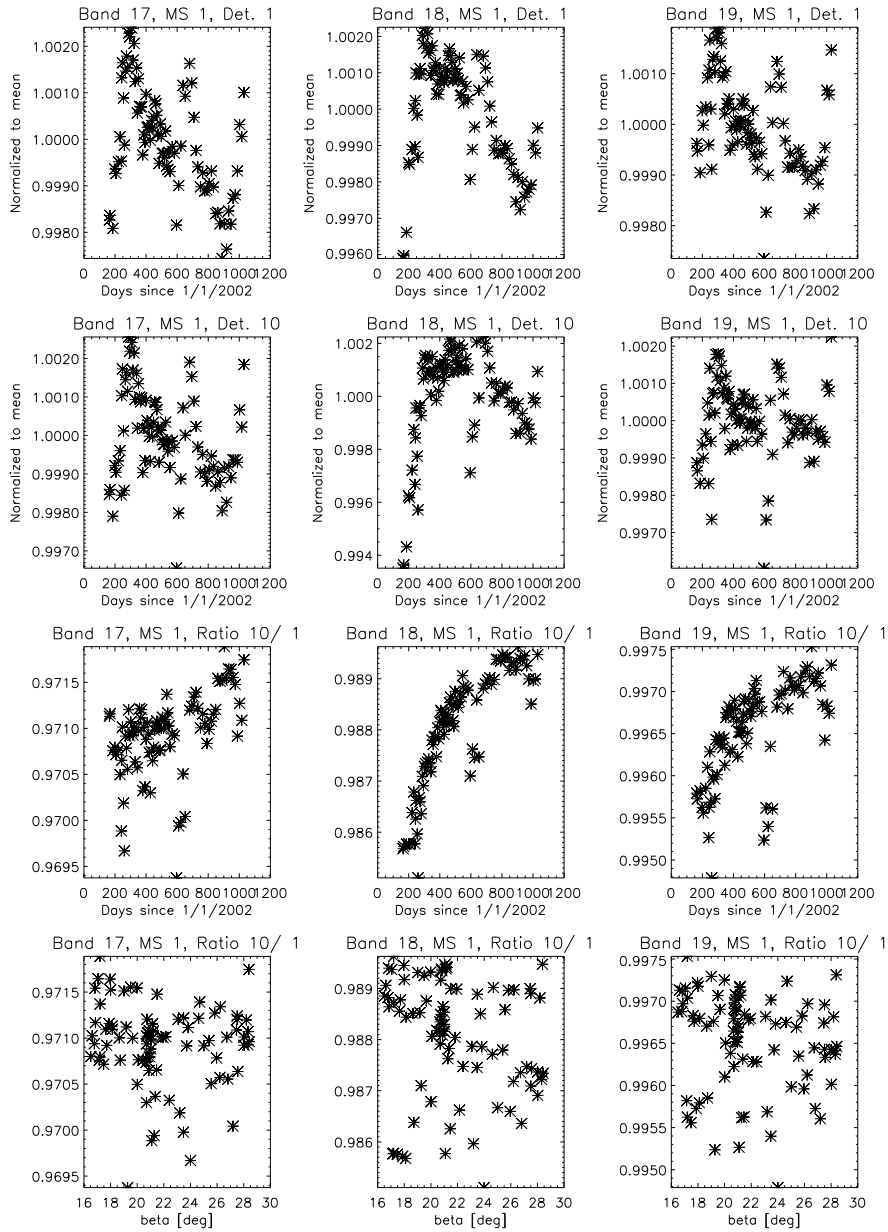












7 Appendix B: LUT comparison

The plots in this appendix show the m_1 from the original MCST LUT V5.0.1.0 (blue line) and the modified LUT V5.0.1.0a (red line), for all MODIS Aqua ocean bands, averaged over detectors, for mirror side 1. The plots on the left show the absolute values normalized to 1, the right side shows the ratio. The top plots show the m_1 at the solar diffuser viewing angle (these are the values stored in the LUT, the bottom plots show the m_1 at the lunar viewing angle (calculated with eq. 10). The m_1 in the original MCST LUT were not extrapolated beyond the last m_1 measurement, the plotting routine used in this figure assumed a constant m_1 for the extrapolation, which results in the horizontal blue line in the plots on the left, and produces the steep increase for the extrapolated values in the plots on the right.

